JOURNAL OF FORENSIC SCIENCES

J Forensic Sci, July 2011, Vol. 56, No. 4
doi: 10.1111/j.1556-4029.2011.01778.x
Available online at: onlinelibrary.wiley.com

TECHNICAL NOTE

GENERAL; CRIMINALISTICS

Roberto Cameriere,[1] *Ph.D.; Danilo DeAngelis,*[2] *Ph.D.; and Luigi Ferrante,*[3] *Ph.D.*

Ear Identification: A Pilot Study

ABSTRACT: Although several papers have recently been devoted to establishing the validity of identification using the ear, this part of the human body still remains underexploited in forensic science. The perfect overlap of two images of the same ear is not really possible, but photographs of the ears as a reliable means of inferring the identity of an individual are poorly treated in the literature. In this study, we illustrate a simple, reproducible method, which divides the photograph of an ear into four parts—helix, antihelix, concha, and lobe—by means of a suitable grid of four straight lines. Although the division does not follow exact anatomical features, their edges do join anatomical points which are more easily identifiable. Measurement of certain areas of these parts can be combined to produce a code allowing personal identification. This method produces false-positive identifications of <0.2%. Last, the repeatability and reproducibility aspects of the method are tested.

KEYWORDS: forensic science, ear, earmark, identification, code number, multivariate beta distribution

Identification by comparing various parts of the body is a normal procedure in forensic work. In particular, fingerprints, frontal sinuses, palatine rugae, bitemarks, and the spinal column have all been used. Although identification by means of ear prints and sometimes video images of ears have been used in court, it is normally rejected because, as the Dutch Court of Appeal stated: "It is the court's opinion that the result of the [ear identification] inquiry finds insufficient support in accepted evidentiary principles."

As early as 1896, in his volume *Signaletic instructions including the theory and practice of anthropometrical identification* (1), Bertillon stated that every part of the human anatomy, including the ear, was so unique that any individual could be identified if that part of the body was properly measured and compared.

Several papers (2–15) have been devoted to ascertaining the validity of identification using the ear, in particular ear prints. Most of them refer to the reliability of earmark identification according to a matching process of the contours of ear structures and comparisons of anatomical annotations by means of sophisticated computer programs.

The most important studies using photographs of ears for identification purposes were developed from the work of Iannarelli (16), who became interested in them in 1948 and, over the next 14 years, classified about 7000 ears from photographs. He created a 12-point measurement scale called the "Iannarelli System," in which the right ear of individuals is specially aligned and normalized with the photographs. Images are normalized by enlarging them until they fit the predefined template. The distance between each of the numbered points is measured and assigned an integer distance value. One possible criticism is the method is not always suitable because of possible difficulties in locating the right anatomical points, particularly the first one. In fact, if the first point is not defined accurately, none of the measurements are useful.

In 2001, Hoogstrate et al. (17) published a paper about ear identification from surveillance camera images and carried out a small-scale experiment with forensically trained and nontrained persons. The results encouraged the method proposed, especially for subjects with forensic experience. The aim of the present study was, following Iannarelli's work (16), to analyze the simplest, minimal, and most easily reproduced anatomical features of the ear useful for personal identification by means of surveillance camera images. We did not follow exact anatomical features, which are often difficult to locate, but chose anatomical points that could be identified without the risk of error. We also looked for a theoretical multivariate distribution of helix, concha, lobe, and antihelix (expressed as proportions of the ear) and the certainty of reproducibility of inter- and intra-observer measurements.

Materials and Methods

Subjects

Ear photographs of Italian subjects (105 women, 118 men) aged between 18 and 60 were analyzed. Subjects with ear malformations or wearing earrings, and cases of fuzzy or unclear photographs were excluded. All subjects were asked to consent to a study of their ears, and only ears were photographed, to guarantee anonymity.

Photographs were taken on a Nikon D40× digital reflex camera (3872 pixels on *x*-axis and 2592 on *y*-axis; shutter speed ≤1/60 sec; Nikon Corp., Tokyo, Japan). No flash was used, only natural reflected light, and attempts were made to avoid the presence of any large shadows. Volunteers were photographed at a distance of about 2 m (focal length 31 mm) in norma lateralis profile. Images were saved in jpg format with low compression (high quality); no image processing was applied, except for rotating the canvas and cropping.

Figure 1 shows the anatomical features of the outer ear. Some of these (e.g., Darwin's tubercle) are not always present; others (e.g., lobule, helix) sometimes did not have clear outlines.

[1]Institute of Legal Medicine, University of Macerata, Via Don Minzoni 9, 62100 Macerata, Italy.
[2]Laboratorio di Antropologia e Odontologia forense (LABANOF), Institute of Legal Medicine, University of Milan, Via Mangiagalli 37, 20133 Milano, Italy.
[3]Department of Clinical Medicine and Applied Biotechnology, Polytechnic University of Marche, Ancona, Via Tronto 10/A, 60100 Ancona, Italy.

Received 19 April 2009; and in revised form 4 Jan. 2010; accepted 15 Feb. 2010.

FIG. 1—*Anatomical features of outer ear: (a) tragus; (b) crus of helix; (c) lower crus of antihelix; (d) triangular fossa; (e) upper crus of helix; (f) helix; (g) Darwin's tubercle; (h) scaphoid fossa; (i) upper concha; (j) antihelix; (k) lower concha; (l) antitragus; (m) lobule; and (n) inter-tragic notch.*

Ear images were recorded and processed with a computer-aided drafting program (Adobe Photoshop 7; Adobe Systems, Inc., San Jose, CA). Ear orientation and determination of helix, antihelix, concha, and lobe edges were obtained by the technique described below.

Ear images were examined at high magnification, to follow the edges of the area of interest with the polygonal tool (moving from point to point on the profile, so that the selected edge corresponded to a straight line drawn by the polygonal tool between two clicks).

The starting picture was an image of the left or right ear from the norma lateralis profile of a subject. To divide the image reproducibly, a grid of four straight lines is drawn (Fig. 2):

- Line r, passing through the starting point of the lobe (A) and the point of junction of the helix with the head (B).
- Line s, parallel to r and tangential to the most posterior part of the concha, located at point C.

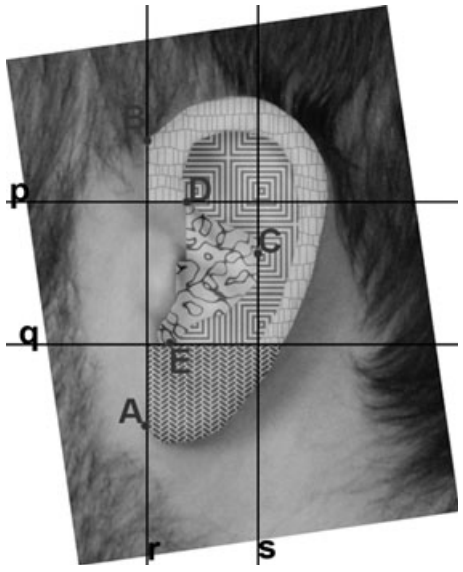

FIG. 2—*Ear image divide by a grid of straight lines p, q, r, and s.*

- Line p, orthogonal to r and passing through point D, that is, the intersection between inferior crux and helix.
- Line q, parallel to p and tangential to the lowest part of the concha (point E).

The ear image is subdivided into its four parts, as follows:

- HELIX: the subset of the morphological helix, bounded frontally by the segment from the intersection of lines p and r and point D, and inferiorly by lines q and s (pattern of vertical "bricks" in Fig. 2).
- ANTIHELIX: the subset of the morphological antihelix, bounded above and posteriorly by the helix and inferiorly by line q to point E; frontally, its edge is represented by the posterior concha profile (pattern of concentric squares in Fig. 2).
- CONCHA: the morphological concha (pattern of intersecting curved lines in Fig. 2).
- LOBE: the subset of the morphological lobe, bounded above by line q and anteriorly by line r ("tyre mark" pattern in Fig. 2).

Figure 3 shows an ear image subdivided into these four parts by means of the grid of lines p, q, r, and s.

The four areas were identified according to Iannarelli's scale (16) and defined by the polygonal lasso instrument of Adobe Photoshop 7 software.

The pixels of the four areas were computed by Adobe Photoshop and presented in the histogram tool.

To determine the number of pixels in each selection (then divided by the number of all pixels representing the whole ear, to obtain a relative surface measurement), we used the "pixel" indication in the histogram palette of Adobe Photoshop CS2 (17). To take into account the effects of possible differences in magnification and angulation among images, measurements were normalized by dividing them by the total area of the ear. Consequently, the measurements of the four variables, helix, antihelix, concha, and lobe, were obtained as proportions of the ear. Last, the outer ear of a given subject was identified by a code number of 8 digits, obtained by rounding off the four proportions to the integer numbers of two digits and putting them in the following order: helix, antihelix, concha, and lobe. For instance, an ear with helix = 15.4, antihelix = 52.7, concha = 15.6, and lobe = 16.3 gives code number 15531616.

Measurements were carried out by two different observers. Assessment of intra- and inter-observer reproducibility was checked on an independent sample of 40 randomly chosen photographs (20 male and 20 female subjects). Within-source variability was assessed by comparing the code numbers obtained by the same rater with two different photographs of the same ear in a random sample of 21 ears.

Statistical Analysis

Intra- and inter-observer reproducibility was assessed by the concordance correlation coefficient. Pearson's correlation coefficients were evaluated between each pair of the four variables characterizing the ear.

The density functions of the multivariate distribution of helix, concha, lobe, and antihelix (expressed as proportions of the ear) were estimated according to the trivariate beta distribution family, the density of which may be written as:

$$f(y_1, y_2, y_3) = \frac{\Gamma(p_1, p_2, p_3, p_4)}{\Gamma(p_1)\Gamma(p_2)\Gamma(p_3)\Gamma(p_4)} y_1^{p_1-1} y_2^{p_2-1} y_3^{p_3-1} \times (1 - y_1 - y_2 - y_3)^{p_4-1}$$

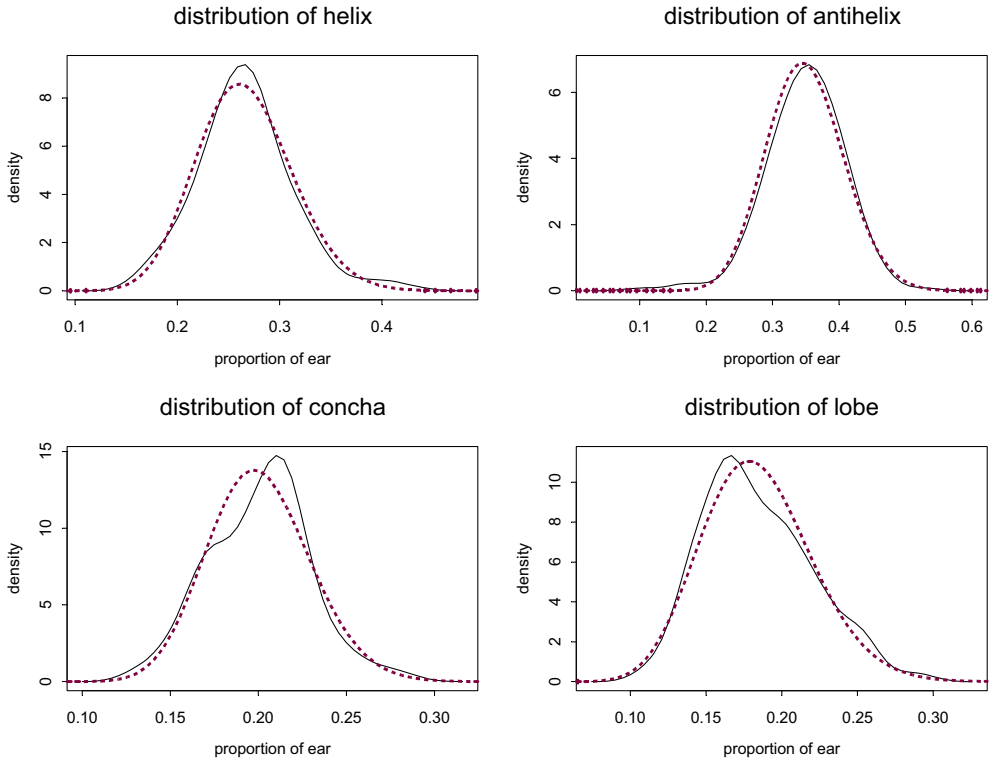

FIG. 3—*Observed distributions of helix, antihelix, concha, and lobe (continuous lines) and corresponding univariate beta distributions (dotted lines).*

where $\Gamma(x)$ is the gamma function, y_1 the helix fraction of the ear, y_2 the concha fraction, and y_3 the lobe fraction, respectively, with $y_i \geq 0$ $i = 1,2,3$; and $\sum_{i=1}^{3} y_i \leq 1$. Clearly, the antihelix fraction may be obtained as $y_4 = 1 - y_1 - y_2 - y_3$.

Let us consider the image of a given ear with a code number, obtained by rounding off the four proportions y_i, $i = 1,..4$; to the integer numbers of two digits. A second ear image of a different individual produces the same code number if its proportions of helix, concha, and lobe differ from y_1, y_2, and y_3 by <0.005. Consequently, the probability that two ear images of different individuals are identified as belonging to the same individual (i.e., false-positive identification) may be estimated as:

$$\int_R f(x_1, x_2, x_3) dx_1 dx_2 dx_3$$

where

$$R = \{(x_1, x_2, x_3) \in [0,1]^3 : |x_i - y_i| < 0.005\}$$

Kolmogorov–Smirnov statistics were used to evaluate the goodness-of-fit and accuracy of model predictions. The intra- and inter-observer reproducibility of all measurements was studied by means of the concordance correlation coefficient, ρ_c. Statistical analysis of data and related graphs was carried out with the S-PLUS 6 statistical program (S-PLUS® 6.1 for Windows, professional edition, Release 1; TIBCO Software, Inc., Palo Alto, CA) and the Microsoft Excel® program (Microsoft Corp., Redmond, WA). The significance level was set at 5%.

Results

With regard to the reproducibility of helix, antihelix, concha, and lobe measurements made separately, the estimated concordance correlation coefficient was $\rho_c > 0.952$ for both observers 1 and 2, and $\rho_c > 0.946$, when the measures of both observers were compared. These ρ_c values did not reveal significant intra- or inter-observer effects ($p > 0.1$), indicating substantial homogeneity of evaluation. With regard to the repeatability (intra-observer reliability) of the code number, no different code numbers between the first and second observations were found. However, with regard to the reproducibility (inter-observer reliability), one different code of 40 comparisons (2.5%) was ascertained. Among the 21 pairs of photographs examined, the code numbers obtained from two photographs of the same ear did not reveal any difference. With Pearson's correlation test with a threshold of significance of 5% showed that the antihelix is significantly correlated with all the other variables and that there is a weak but significant correlation between concha and lobe, whereas helix + concha and helix + lobe are not significantly correlated (Table 1).

As the four variables are related by the identity: helix + antihelix + concha + lobe = 1, we chose the three less well-correlated variables for identification, that is, the helix, concha, and lobe. The parameters of the joint distribution of these variables were estimated by the maximum likelihood procedure and are listed in Table 2. Statistical analysis showed that the difference of estimated parameters between sexes was not significant ($p = 0.6$).

The Kolmogorov–Smirnov test (Table 3) showed that the above-hypothesized beta distribution functions and their corresponding empirical ones did not differ significantly ($p > 0.30$), indicating that the assumed beta distribution functions matched observations well (Fig. 4). Trivariate beta distribution was used with the estimated parameters (Table 2) to evaluate the probability that two different individuals have the same code number (false-positive identification). This probability was found to be <0.002.

Discussion

In recent years, identification of individuals by their ears has been studied with particular attention to methods of earmark analysis.

Most of the methods applied have developed reliable but very complex image processing techniques (4), which are difficult to use without suitable computer programs.

TABLE 1—*Pearson's correlation coefficients between helix, antihelix, concha, and lobe.*

	Helix	Antihelix	Concha	Lobe
Helix	1			
Antihelix	−0.697	1		
Concha	−0.079	−0.318	1	
Lobe	−0.112	−0.441	−0.194	1

TABLE 2—*Maximum likelihood estimates of parameters of beta distribution.*

Parameters	Estimate	SD	*T*	*p*-Value
p_1	26.55	1.46	18.2	<0.001
p_2	20.24	1.10	18.4	<0.001
p_3	18.45	1.02	18.1	<0.001
p_4	34.68	1.95	17.8	<0.001

TABLE 3—*Results of Kolmogorov–Smirnov (KS) goodness-of-fit test to ascertain whether empirical distribution of helix, antihelix, concha, and lobe may be considered as beta distributions.*

Variable	KS statistics	*p*-Value
Helix	0.057	0.47
Antihelix	0.055	0.52
Concha	0.062	0.36
Lobe	0.065	0.30

To the best of our knowledge, few papers focus on identification of individuals according to photographs of their ears.

In his seminal paper, Iannarelli (16) proposed a new method based on measurement of the distances between some anatomical points. However, the locations of these points, particularly the first, are difficult to ascertain, with a consequent increase in inter-observer variability.

As in the majority of biometrics identification methods (e.g., earprints/earmarks, fingerprints, facial recognition, and DNA evidence), also in the field of identification of ear photographs, categorical conclusions on uniqueness are difficult to sustain from a scientific viewpoint, even when direct overlapping of two ear images is carried out.

Although the technique based on the overlap of two ear images would be considered the easiest and conclusive method to identify an ear, it may suffer from slight intra-subject variability of ear photographs, for example, because of age-related modifications (17) or because of the differences between their magnification, lighting, and pose variations.

Furthermore, the quality of the "distance" from the actual three-dimensional organ to its two-dimensional image must always be taken into account, as must the loss of information of the image. In addition, unsuccessful overlapping may produce a significant number of false negatives, unless we are willing to accept a certain degree of tolerance, which can be defined in terms of the probability of false negatives and false positives.

With regard to the identification of men by ear photographs, Hoogstrate et al. (17) stressed the importance of collecting as many observations as possible and checking whether ears can be distinguished from each other at a certain level of measured or observed accuracy. However, the authors concluded by stating that the uniqueness of ears can only be inferred after developing a model for external ear patterns and estimating the probability of occurrence of uniqueness in the population. Following this line, we modeled the distribution of helix, concha, lobe, and antihelix, expressed

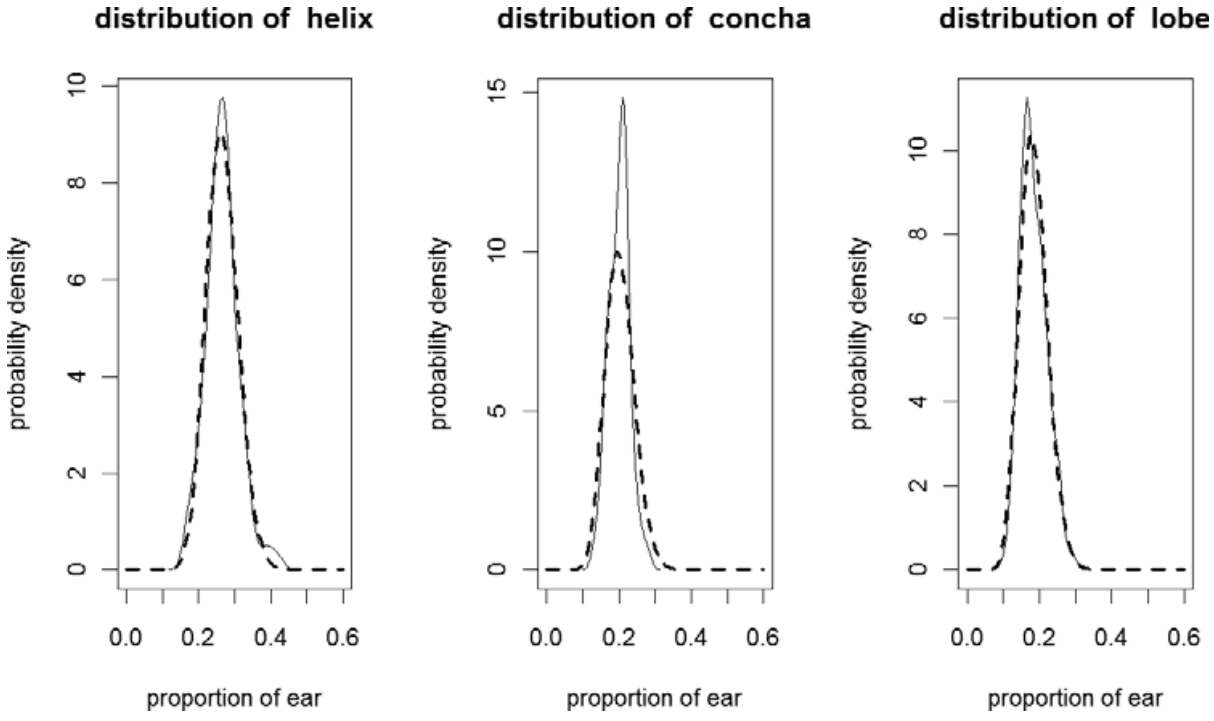

FIG. 4—*Observed distributions of helix, antihelix, concha, and lobe (continuous lines) and corresponding univariate beta distributions (dotted lines).*

as proportions of the ear, according to a trivariate beta distribution, which appear to be an appropriate statistical model for our data.

In this study, we propose a technique for individual identification based on a few simple, reproducible anatomical features of the ear. With regard to false positives, our method shows high specificity, although only a small number of anatomical features are examined.

Possible future development along these lines may be foreseen—first, evaluating the difference between a closed set or an open set. Therefore, the importance of differences in camera model, position, quality of images, etc., is obvious. The results and the ease with which the limited number of anatomical features can be evaluated encourage us to use our method to identify ear images that come from surveillance camera images.

For instance, the method proposed here can be implemented with further qualitative features, such as Darwin's tubercle, moles, piercings, and other minutiae.

References

1. Bertillon A. Signaletic instructions including the theory and practice of anthropometrical identification. New York, NY: The Werner Company, 1896.
2. Alberink I, Ruifrok A. Repeatability and reproducibility of earprint acquisition. J Forensic Sci 2008;53:325–30.
3. Alberink IB, Ruifrok AC, Kieckhoefer H. Interoperator test for anatomical annotation of earprints. J Forensic Sci 2006;51:1246–54.
4. Alberink I, Ruifrok A. Performance of the FearID earprint identification system. Forensic Sci Int 2007;166:145–54.
5. Rutty GN, Abbas A, Crossling D. Could earprint identification be computerised? An illustrated proof of concept paper. Int J Legal Med 2005;119:335–43.
6. Abbas A, Rutty GN. Ear piercing affects earprints: the role of ear piercing in human identification. J Forensic Sci 2005;50:386–92.
7. Meijerman L, Sholl S, De Conti F, Giacon M, van der Lugt C, Drusini A, et al. Exploratory study on classification and individualisation of earprints. Forensic Sci Int 2004;140:91–9.
8. Victor B, Bowyer K, Sarkar S. An evaluation of face and ear biometrics. In: Kasturi R, editor. Proceedings of the 16th International Conference on Pattern Recognition; 2002 Aug 11-15; Quebec City, Canada. Los Alamitos, CA: IEEE Computer Society Press, 2002;429–32.
9. Chang K, Bowyer KW, Sarkar S, Victor B. Comparison and combination of ear and face images in appearance-based biometrics. IEEE Trans Pattern Anal Mach Intell 2003;25:1160–5.
10. Moreno B, Sánchez Á, Vélez JF. On the use of outer ear images for personal identification in security applications. In: Sanson LD, editor. Proceedings of the IEEE 33rd Annual International Carnahan Conference on Security Technology; 1999 Oct 5–7; Madrid, Spain. IEEE Explore Digital Library, 1999;469–76, http://ieeexplore.ieee.org/xpl/freeabs_all.jsp?arnumber=797956 (accessed April 4, 2011).
11. Burge M, Burger W. Ear biometrics. In: Jain A, Bolle R, Pankanti S, editors. Biometrics: personal identification in a networked society. Norwell, MA: Kluwer Academic, 1998;273–86.
12. Burge M, Burger W. Ear biometrics in computer vision. In: Sanfeliu A, editor. Proceedings of 15th International Conference of Pattern Recognition; 2000 Sept 3–7; Barcelona, Spain. Los Alamitos, CA: IEEE Computer Society Press, 2000;826–30.
13. Hurley DJ, Nixon MS, Carter JN. Automated ear recognition by force field transformations. Proceedings of IEEE Colloquium on Visual Biometris; 2000 March 2; London, UK.: IEEE Explore Digital Library, 2000; 7/1-7/5, http://ieeexplore.ieee.org/xpl/freeabs_all.jsp?arnumber=847018 (accessed April 4, 2011).
14. Hurley DJ, Nixon MS, Carter JN. A new force field transform for ear and face recognition. Proceedings of the IEEE 2000 International Conference on Image Processing; 2000 Sept 10–13; Vancouver, BC, Canada: IEEE Explore Digital Library, 2000;25–8, http://www.ieee.org/portal/innovate/search/article_details.html?article=900883 (accessed April 4, 2011).
15. Champod C, Evett IW, Kuchler B. Earmarks as evidence: a critical review. J Forensic Sci 2001;46:1275–84.
16. Iannarelli A. Ear identification, forensic identification series. Fremont, CA: Paramount Publishing Company, 1989.
17. Hoogstrate AJ, Van Den Heuvel H, Huyben E. Ear identification based on surveillance camera images. Sci Justice 2001;41:167–72.

Additional information and reprint requests:
Roberto Cameriere, Ph.D.
Institute of Forensic Medicine
University of Macerata
Via Don Minzoni 9
62100 Macerata
Italy
E-mail: r.cameriere@unimc.it